Chapter 5

Charge Transfer Induced Magnetism in Mixed-stack Complexes

In this chapter ferromagnetism in mixed-stack charge-transfer (CT) complexes is explained and evaluated through new theoretical framework of our own. In DFT framework, broken symmetry (BS) approach is adopted to evaluate J using spin projection technique. No overlap between singly occupied molecular orbitals (SOMOs) suggests a through-space ferromagnetic interaction between the donor and the acceptor in the ground state of the complexes. Apart from the ground state, the magnetic status of the molecules is studied by varying interlayer distance d, the extent of slippage (slipping distance r, r′, and deviation angle α), and rotational angle θ, which play a crucial role in magneto-structural correlation. Furthermore, it is categorically observed that the ferromagnetic interaction reaches its zenith at minimum energy crystallographic stacking mode resulting in maximum value of coupling constant in the ground state.

5.1 Introduction

In recent decades, a considerable number of magnetically active stacked materials have been isolated and characterized where the magnetic interaction is set in through intra-stack charge transfer (CT).[1] The possibility of such intermolecular magnetic interaction in organic compounds was first reported by McConnell.[2] His theoretical idea was instrumental for synthesis and characterization of a new class of organic CT compounds; namely, stacked CT systems.[3] Stacked CT complexes are classified into segregated-stack (...DDD..., ...AAA...) and mixed-stack (...DADADA...) type, where D and A imply donor and acceptor respectively. The segregated-stack CT complexes are widely known because of their high conductivity. Furthermore, a few segregated-stack CT complexes are known to show superconductivity.[3] On the other hand, mixed-stack CT complexes are also very fascinating materials because of their unique properties such as non-linear electrical conduction,[4] electronic phase transition,[5] magneto-lattice transition,[6] non-linear optical effects,[7] neutral-ionic phase transition[8] and magnetism.[9] Because of the versatile applicability of the mixed-stack CT complexes, a large number of such materials are synthesized and characterized.[10] Multifarious behavior of such type of complexes relies strongly upon non-covalent charge transfer interactions between the donors and the acceptors.[11]

Understanding of magnetic behavior in mixed-stack CT systems is of primary importance to tune such materials for desired applications. McConnell proposed a second model of ferromagnetic spin alignment using ionic CT salts.[12] The concept of superexchange ferromagnetism was extended to the domain of organic CT solids, which was initially used to explain magnetic behavior in inorganic systems.[13] Breslow and coworkers proposed a mechanism for ferromagnetic interaction in charge transfer donor-acceptor complexes where the spins on neighboring species are in parallel fashion, so that charge transfer can lead to the favored triplet state in one of the partners in the CT systems.[14] According to Miller and coworkers,[1a,15] the ferromagnetic interaction between decamethylferrocene (DMeFc) and tetracyanoethylene (TCNE) in $(DMeFc)^{+\bullet}(TCNE)^{-\bullet}$ complex is due to electron hopping (resonance interaction) between one of the orbitals in the triply occupied doubly degenerate manifold on $(DMeFc)^{+\bullet}$ and the singly occupied orbital on $(TCNE)^{-\bullet}$. Through *ab initio* study, it has been found that the coulombic exchange between the $2p\sigma$ orbital of triplet methylene and the

π molecular orbital of the nitroxyl radical is the origin of ferromagnetic interaction in mixed clusters of methylene and nitroxyl radicals.[16] It has been suggested that the concept of zero or minimal overlap between the singly occupied molecular orbitals (SOMOs) should play a more fundamental role in the optimization of ferromagnetism. A study on magnetic properties in phenalenyl radical dimer highlights the effect of stacking mode on magnetic interaction.[17] In the DFT framework, Ni et al. studied the magnetic switching depending upon the stacking pattern.[18] They showed that the cooperative effect of the weak intermolecular bonding between the layers is responsible for the magnetic phase transition.

Though mixed-stack CT complexes usually show antiferromagnetic interaction,[9h,19] Nakajima et al. recently synthesized two mixed stack complexes namely, (1) (HMTTF)[Ni(mnt)$_2$] (HMTTF = bis(trimethylene)-tetrathiafulvalene, mnt = maleonitrile dithiolate) and (2) (ChSTF)[Ni(mnt)$_2$] (ChSTF = 2,3-cyclohexylenedithio-1,4-dithia-5,8-diselenafulvalene) which are reported to be the first of their own kind to show ferromagnetic interaction.[20] From temperature dependent g value and susceptibility curve, these two compound are found to have several magnetic transitions at different temperatures. Compound 1 and 2 exhibit a peak in their susceptibility curbe at 8K and 16K respectively, showing ferromagnetic interaction. The ESR spectra of these complexes give a single Lorenzian in the whole temperature range without separating the donor and acceptor spins, which indicates the presence of exchange interaction between the spins. Because Nakajima et al. describe the origin of ferromagnetism in these nixed-stack complexes to be enigmatic, in the present work, we put our effort to find out the nature and reason of magnetic interaction in the same two complexes isolated by Nakajima et al.[20] While doing so the mixed-stack face to face donor acceptor pair of the complexes taken from the crystallographic file is chosen as the reference to study their magnetic behavior. As the magnetic interaction in such CT complexes is subject to *a priori* donor to acceptor charge transfer, the ferro- or antiferro-magnetic behavior will also depend upon the charge transfer.[21] From a variety of mechanisms suggested for donor to acceptor charge transfer, two basic propositions can be figured out which fit best for CT systems.[22] The first is the electron transits through bond (TB), a suitable pathway built from the nonorthogonal molecular orbitals (MOs) of the donor and the acceptor pair.[22, 23] Overlap of nonorthogonal MOs facilitate antiferromagnetic interaction. However, in case of the absence of such overlap, the travelling electron has to tunnel through-space (TS) and it encounters a potential energy barrier.[24]

In some specific cases, there may also be a quantum interference between these two pathways (TB and TS).[25] However, neither TB nor TS electron tunneling is sufficient alone to properly address a CT process and these pathways often occur synchronously.[23b] This sets the crux of the present investigation, which is divided in two parts. First, an effort is made to understand the mechanism of magnetic interaction in (1) (HMTTF)[Ni(mnt)$_2$] (HMTTF = bis(trimethylene)-tetrathiafulvalene, mnt = maleonitrile dithiolate) and (2) (ChSTF)[Ni(mnt)$_2$] (ChSTF = 2,3-cyclohexylenedithio-1,4-dithia-5,8-diselenafulvalene), two mixed-stack ferromagnetic CT complexes recently synthesized by Nakajima et al.[20] HMTTF and ChSTF are the donor and the Ni(mnt)$_2$ is the acceptor in these two complexes. The role of charge transfer behind their magnetic nature is investigated and the charge transfer energy is correlated with magnetic interaction. The approximate spin projection method of Yamaguchi is employed to quantify the magnetic interaction in terms of exchange coupling constant (J).[26] This value is compared with the extent of coupling constant derived through the use of charge transfer energy and spin densities of donor and acceptor sites. The interaction among molecular orbitals is fundamental to describe magnetic behavior in any molecular system. According to Hoffmann, a triplet state is stabilized when the overlap between two SOMOs is small, whereas singlet state predominates when the overlap is large.[27a] Ferromagnetic interaction between two open shell molecules takes place when the molecules are arranged in such a way that two SOMOs are orthogonal or as nearly so as possible. In traditional inorganic magnets, the nodal properties of d or f orbitals would lead to the cancellation of overlap in their crystals. In case of organic molecules, the proper geometrical arrangement is crucial for cancellation of overlap, as they only have $2p$ atomic orbitals.[16] Present systems involve metal d orbitals as well as p orbitals of nonmetal. Thus the arrangement of SOMOs, centered on different units, becomes an important factor to determine the nature of the magnetic interaction. Hence, in the second part of this work, a magneto-structural correlation in the reference systems is explored to know whether the molecules show ferromagnetic interaction by cancellation of overlap or not. The stacking pattern of the molecules is modified by changing the rotational angle between donor and acceptor units.

5.2 Theoretical Details and Computational Methodology

The interaction between two magnetic sites 1 and 2 is generally expressed by Heisenberg spin Hamiltonian $\hat{H} = -J\hat{S}_1 \bullet \hat{S}_2$, where $\hat{S}_1$ and $\hat{S}_2$ are the respective spin angular momentum operators and J is the exchange coupling constant. Since, the Heisenberg Hamiltonian is simply related to spin eigenfunctions, it becomes necessary to map the eigenvalues and eigenfunctions of an exact nonrelativistic Hamiltonian into the spin Hamiltonian. Moreira and Illas have shown that for an interaction between two spin-1/2 sites, it is possible to map the Heisenberg eigenstates to the triplet and singlet N-electron states and the coupling constant can be derived from the singlet-triplet energy difference.[27b] The positive value of J indicates the ferromagnetic interaction while the negative value signifies the antiferromagnetic interaction between two magnetic sites. Broken symmetry (BS) approach given by Noodleman[28] in DFT framework is useful to evaluate J in cases of weak or no overlap between magnetic orbitals. The expression put forward by Bencini, Ruiz and co-workers uses the energy of the BS state as that of open shell singlet at stronger overlap limit of magnetic orbitals.[29, 30] However, the spin projected method, [31] coined by Yamaguchi[26] (eq 1) is applicable in any overlap limit and hence used in this work to evaluate the coupling constant (J_Y),

$$J_Y = \frac{E_{BS} - E_T}{\left\langle \hat{S}_T^2 \right\rangle - \left\langle \hat{S}_{BS}^2 \right\rangle}. \qquad (5.1)$$

Here, E_{BS} and E_T are the energies of the BS and triplet state respectively, whereas $\left\langle \hat{S}_T^2 \right\rangle$ and $\left\langle \hat{S}_{BS}^2 \right\rangle$ represent the average spin square values of triplet and BS states respectively.

As discussed in the introduction, the donor-acceptor magnetic coupling is induced by electron transfer from donor to acceptor. There have been several efforts to theoretically model such charge transfer.[22] Among these, a perturbative treatment has widely been adopted to account for the electron tunneling process.[32] Anderson in his pioneering work, derived the second order perturbation energy (ΔE) for such an intersite charge transfer and correlated this energy with magnetic interaction as,[33]

$$\Delta E = \frac{t_{ij}^2}{U}\left(\frac{1}{2} + 2\hat{S}_i \bullet \hat{S}_j\right). \tag{5.2}$$

Here, t_{ij} is the hopping integral which carries an electron from site i to site j and U is the single ion repulsion energy. However, this t^2/U term is well-known in the Hubbard model and related to the coupling constant (J).[34] In their seminal works, Calzado et al. applied *ab initio* CI techniques to compute these individual contributions to the magnetic coupling constant using effective Hamiltonian theory.[35] However, in of our recent studies, instead of direct estimation of this t^2/U term; the above expression was modified to estimate the coupling constant in terms of the second order perturbation energy (ΔE) for charge transfer between sites and spin density on those centers (ρ_i and ρ_j).[36] This coupling constant emanates from the charge transfer from donor to acceptor, and hence referred to as J_{CT},

$$J_{CT} = \frac{2\Delta E}{1 + \rho_i . \rho_j} \tag{5.3}$$

In a model proposed by Heitler and London, J is split into ferro- and antiferro-magnetic contributions

$$J = K + 2\beta S. \tag{5.4}$$

The first part, being the two-electron exchange integral, is necessarily positive. Whereas the second part contains resonance integral (β) and an overlap integral (S), which are of opposite sign and thus their product becomes negative. Hence, the value of overlap integral plays a crucial role in controlling the overall nature of magnetic interaction.[37]

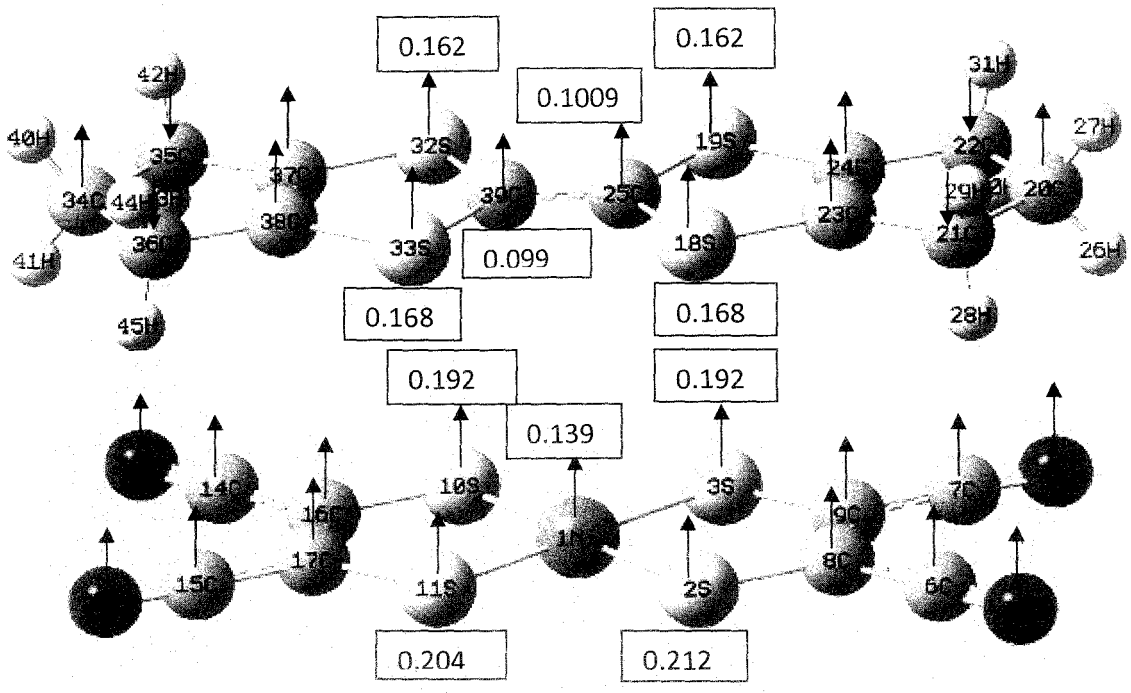

(HMTTF)[Ni(mnt)$_2$] (1)

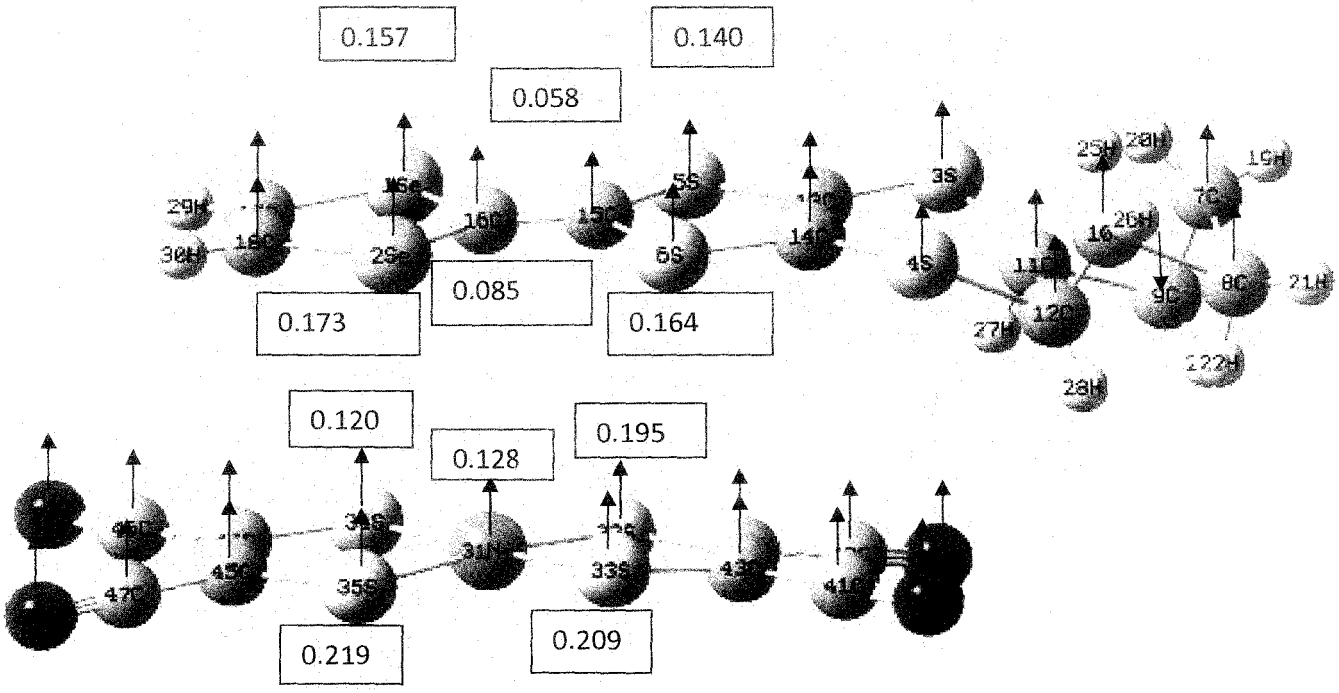

(ChSTF)[Ni(mnt)$_2$] (2)

Figure 5.1 Systems under investigation with major spin densities on individual atoms in triplet ground state at UB3LYP/LANL2DZ level of theory.

The orbital overlap between magnetic orbitals ($\psi_i^{\pm}$), $T_i = \langle \psi_i^{+} | \psi_i^{-} \rangle$ can approximately scale the spin delocalization; which is estimated by the following relationship:

$$T_i = n_i - 1,\ T_i = 1 - n^*_i, \tag{5.5}$$

where n_i and n^*_i are the occupation number of bonding and antibonding natural orbitals (NO), T_i = 0 for pure diradical and T_i = 1 for closed shell pair.[38]

The geometries of systems under investigation are taken from the crystallographic structures obtained from reference 20 (Figure 5.1). Hybrid functional B3LYP is known to be effective for evaluation of magnetic exchange coupling constant in molecular systems.[39] Therefore, in this work we rely on B3LYP functional, coupled with LANL2DZ basis set in the unrestricted framework for assessing the magnetic behavior of the complexes. The B3LYP functional and LANL2DZ basis set also known to produce satisfactory results for the calculation of different properties of complexes.[40] More accurate Complete Active Space Self-Consistent Field (CASSCF) technique is also carried out on the ground state of the mixed-stack complexes to verify the reliability of DFT methods in estimating proper coupling constant values. Several previous studies have shown that a small active space in the calculation of magnetic exchange coupling using CASSCF is good enough for an accurate description of magnetic interaction.[41] Hence, in this work a CASSCF(4,4) methodology is adopted for the calculation of exchange coupling constant (J_{CAS}). The CASSCF(4,4) method is also used to calculate the occupation number of molecular orbitals through eq 5. This method is capable of considering the effect of HOMO and LUMO in the magnetic interaction between two SOMOs.[42] All calculations are performed using *Gaussian 09W* suite of quantum chemical package.[43]

5.3 Results and Discussion

5.3.1 Magnetic behavior in ground state of the systems

Prior to the charge transfer, the donor fragments of the complexes are in singlet state and the neutral acceptor part is in triplet state because of d^8 configuration of Ni (II). To understand the source and the destination of charge transfer, the Mulliken spin density distribution of the ground states in complex 1 and 2 is computed through DFT (Figure 5.1), which is reported to produce reliable spin density distribution.[44] The figure displays significant positive spin density

on the NiS_4 fragment of the acceptor part which is in accordance with the experimental report.[45] On the other hand, in the donor part, positive spin density relies on the $X_2C\text{-}CS_2$ (X=S, Se) moiety in both the systems. Compared to the neutral singlet state of the donor, the positive spin density on D^+ suggests departure of β-spin from its HOMO. Similarly, the up-spin density in the neutral acceptor reduces in the anionic state due to the acceptance of that β-spin into one of its β-LUMOs, which are the counterpart of α-SOMOs. The β- spin transfer from the donor to the Ni d orbital is also very logical because Ni(II), have more than a half filled d^8 orbital(D) is bound to accept only the system β spin.[36] The presence of almost equal spin parallelly align in the donor and acceptor undoubtedly advocates for the participation of $Ni(mnt)_2$ fragment in the magnetic interaction as also claimed in reference 20 because of larger g value of the complex than should be of TTF or STF only. However, the spin density is not confined in Ni, and is rather dispersed on ligated S atoms (Figure 5.1). This fact is also verified through the comparison of β –HOMO of neutral donor and SOMO diagram in the neutral acceptor (Figure 5.2).

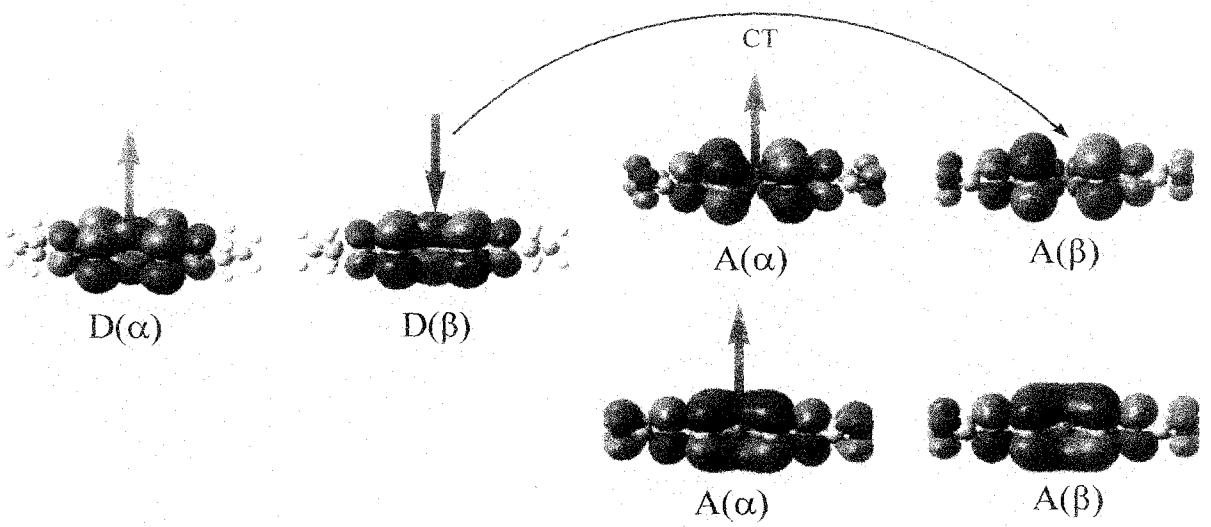

Figure 5.2 Spin transfer from the β –HOMO of neutral donor (D) to the β-LUMO of neutral acceptor (A) with Ni(II) in both the complexes 1 and 2 at UB3LYP/LANL2DZ level.

From the MO diagrams of molecules 1 and 2, it is found that one SOMO is composed by the atomic orbitals solely from the donor and other one is constituted from the contributions from acceptor atomic orbitals only (Figure 5.3). Apart from MO picture, according to Pauling-Slater-

Coulson pictures of bond hybridization and polarization natural bonding orbital (NBO) analysis is a useful tool to provide a quantitative description of intermolecular interactions.[46] The NBO analysis displays a zero overlap between the donor and acceptor in the ground state of these complexes (Appendix 1). Therefore, in can be surmised that the through-space charge transfer is responsible for ferromagnetic interaction (Scheme 5.1). Considering the spin topology of the complex 1 and 2, S and Se atoms in the donor part are recognized as the gateway of charge transfer. On the other hand, it has previously been explained that basically a beta spin transfers from donor to acceptor. Hence, there is no possibility of up spin accumulation on S atoms as a direct consequence of charge transfer.

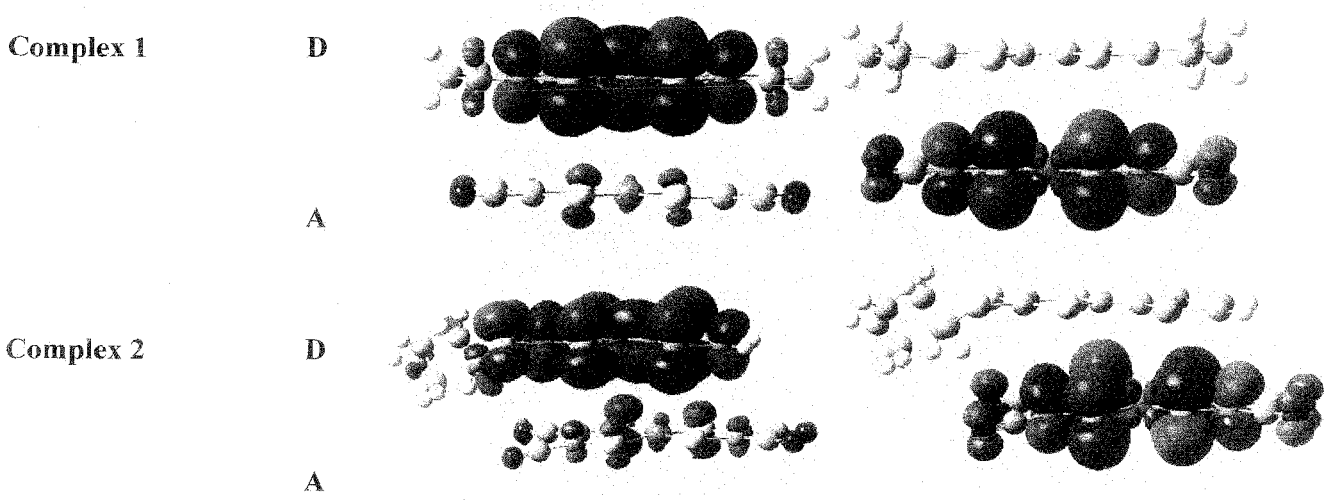

Figure 5.3 SOMOs of the complexes 1 and 2 in their triplet ground state at UB3LYP/LANL2DZ level of theory (isodensity surface value 0.02).

Moreover, in the acceptor moiety the spin density on Ni is reduced to 0.139 in the anionic state compared to the expected spin density of 2 in its neutral state. This observation suggests Ni as the major recipient of the beta spin, which is later dispersed on S atoms. The value of charge transfer energy (ΔE) between these relevant sites in donor and acceptor is taken from the matrix of second order perturbation energy in NBO output. From this ΔE value and spin densities on relevant donor and acceptor sites, the coupling constants for both the complexes are estimated using eq 5.3. The sign and magnitude of coupling constants obtained in this way are found to be in reasonable agreement (Table 5.1) with those estimated through eq 5.1. To further validate

these values of coupling constants, we resort to more accurate CASSCF (4,4) method, which also produces J values with same sign and order of magnitude (Table 5.1).

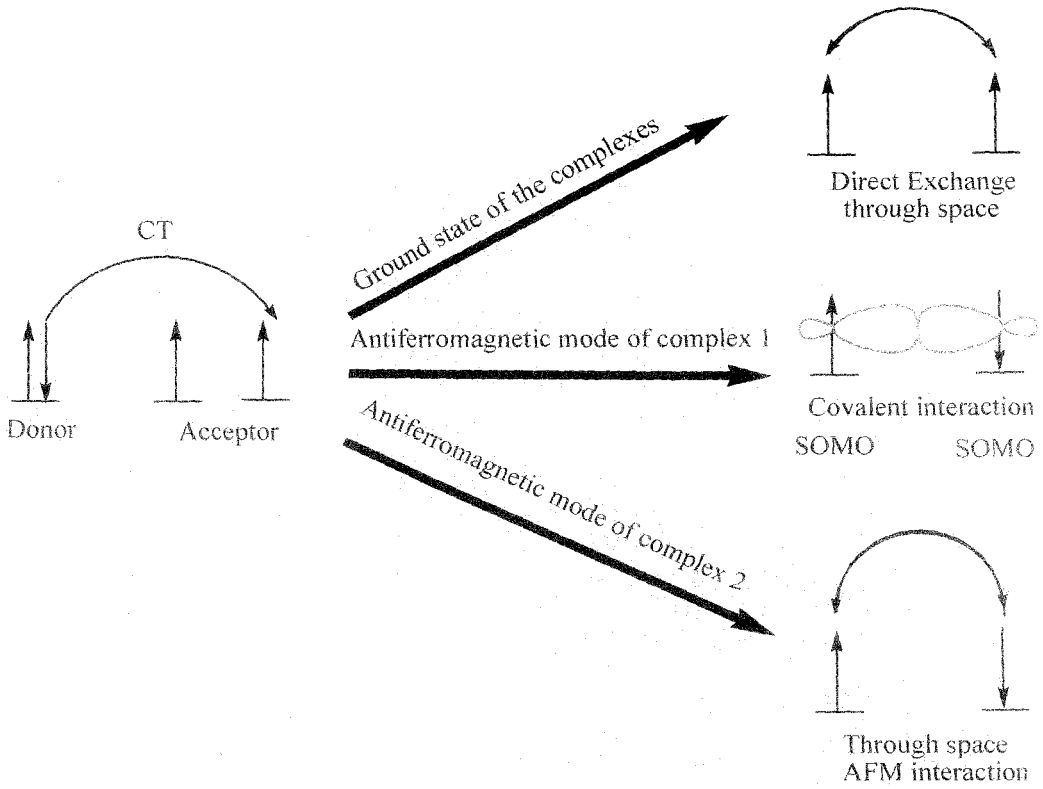

Scheme 5.1 Exchange Coupling Mechanism in Mixed-Stack CT Complexes.

Table 5.1 Comparison of Intermolecular Magnetic Exchange Coupling Constant Values Obtained Through (i) eq 5.1 (J_Y) (ii) eq 5.3 (J_{CT}) at UB3LYP Level and (iii) CAS (4,4) (J_{CAS}) Level of Theory, Using LANL2DZ Basis Set for the Complexes 1 and 2

Complex	J_Y (cm^{-1})	J_{CT} (cm^{-1})	J_{CAS} (cm^{-1})
1	66	68	52
2	70	20	42

The consideration of active space in CASSCF is validated by the similar nature of SOMOs, obtained through CASSCF and DFT (Appendix 1). The ferromagnetic nature of complex 1 and 2 is in qualitative agreement with the experimental results, which proclaim these systems to be the first reported "ferromagnetic mixed-stack complexes".[20] One can further rationalize through-space ferromagnetic interaction between the donor and acceptor SOMOs through their T_{SOMO} values. The T_{SOMO} values of complex 1 and 2 are computed (eq 5.5) in CASSCF(4,4) method, using the occupation number of doubly occupied molecular orbital (DOMO), SOMOs and LUMO, in their triplet ground states. The T_{SOMO} values in both the systems are found to be 0.0 in the triplet state and in turn validate the zero overlap between magnetic orbitals.

5.3.2 Stacking effect of the magnetic interaction

The ordering of magnetic moment and extent of magnetic interaction in transition metal clusters depend on the size of the clusters.[47] Cheng et. al., studied the size dependent magnetic property of Cr clusters. They found that in all the clusters, though the extent of magnetic coupling changes with the cluster size, the antiferromagnetic nature of interaction remains intact.[47] Ni et al.[18] studied the stacking pattern controlled magnetic switching property of $[Ni(mnt)_2]^-$ dimer by taking the face to face pair of $[Ni(mnt)_2]^-$. They had shown that the nature of magnetic property of dimers bears a resemblance to the bulk nature. Following this analogy, among various possibilities of magnetic interaction within the crystal; we study the face to face magnetic interaction among donor-acceptor pair of these complexes. Stacking mode of the complexes is important to understand the magnetic behavior of the system and also to determine the magnetic coupling constant. Yoshizawa and Hoffman[27a] studied the coupling of two diphenylmethyl radicals as a function of its rotational angle (θ) and they conclude that ferromagnetic coupling is favored when θ is close to either 60° or 180° and antiferromagnetic interaction near 120° because the partial overlaps are almost cancelled in 60° and 180° stacking modes due to the nodal structure of the SOMOs.[27a] On the other hand, according to Ni et al.,[18] $[Ni(mnt)]^-$ molecules have maximum ferromagnetic interaction when their corresponding rotational angles are 30° and 60° instead of 60° and 180°. In the present study, in complex 1 and 2, the rotational angles are 53° and 49° which are close to 60° for ferromagnetic complexes. In these values of the rotational angles, complexes 1 complex 2 are found to have minimum energy compared to other arbitrarily chosen rotational angles (Table 5.2). We have estimated the

magnetic exchange coupling constant, varying rotational angle for these two complexes (Figure 5.4). We find that for complexes 1 and 2 the maximum ferromagnetic interaction occurs at rotational angle 53° and 49° respectively which are their corresponding rotational angles found from CIF data.

Table 5.2 The Energy (in a.u.) of the Complexes at Various Rotational Angles (the respective rotational angles are given in parenthesis). The Energy Values are Computed at UB3LYP/LANL2DZ Level

Complex 1	Complex 2
−1237.92407(43)	−1255.80979(43)
−1237.94631(53)	−1255.82236(49)
−1237.92606(59)	−1255.24864(66)
−1237.92250(67)	−1254.87364(70)

With variation in rotational angles in complex 1 and 2, extent of ferromagnetic interaction reduces. As a whole, from Figure 5.4 it is clear that ferromagnetic interactions are more sensitive towards stacking pattern. In one of our recent study, the dependence of the exchange coupling constant on intermetallic distance was investigated for Mn clusters. It has been found that the extent of ferromagnetic coupling is maximum at equilibrium bond distance.[24c] Thus, existing references as well as the present study unanimously advocate that ferromagnetism reaches its zenith at the ground state geometry leading to maximum value of *J*. The intermolecular distance also determines the extent and nature of the magnetic interaction. As for example, in reference 18, the intermolecular distance of ferromagnetic dimer complex of $Ni(mnt)_2^-$ is 3.55Å; whereas the distance is 3.65Å in the antiferromagnetic analogue. In the present work, the intermolecular distance for complex 1 and 2 are found to be 3.63Å and 3.64Å at their ferromagnetic ground state, reported in reference 20 (Figure 5.5). Nearly the same distance between magnetic sites in both the complexes is reflected in the closeness of their *J* values (Table 5.1).

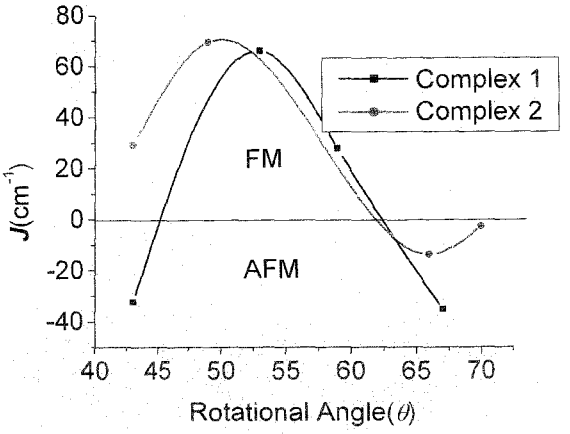

Figure 5.4 Rotational angle (θ) vs. J plot for the complexes in their different stacking mode at UB3LYP/LANL2DZ level of theory.

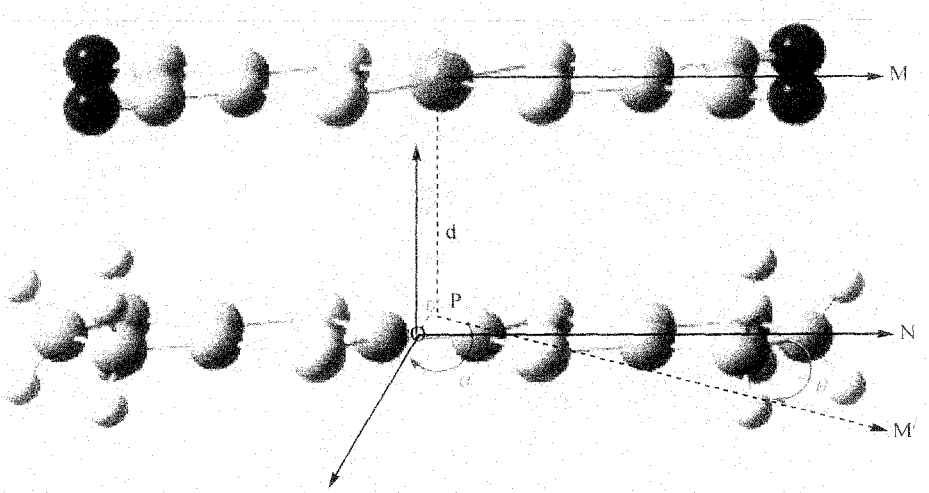

Complex	d(Å)	r(Å)	r'(Å)	θ (°)	α (°)
1	3.63	1.58	0.23	53	0
2	3.64	1.63	0.62	49	3

Figure 5.5 Packing pattern in the complexes (shown with the example of complex 1). M and N are the axes of symmetry of planar monomer and the planar part of the monomer C_2S_4 passing through the metal atoms and C-C bond. The point P and M' are the vertical projections of the upper Ni atom and axis to the lower layer, respectively. The structure of the complex can be parameterized by interlayer distance d, the extent of slippage (slipping distance r, r' and deviation angle α) and rotational angle θ is defined as the angle between P M' and ON.

Next, we investigate the origin of antiferromagnetism in the present systems at a few particular stacking modes, at rotational angles 43° and 67° for complex 1 and 66° and 70° for complex 2. The closest S atoms of two layers are 3.62Å and 3.63Å apart in two AFM stacking modes for complex 1, which are less than their van der Waals radii (3.70Å); i.e., they can form covalent type bond between two layers. From the HOMO diagrams given in Table 5.3, it is clear that in the antiferromagnetic stacking modes of complex 1, there is an overlap between donor and acceptor fragments, which facilitates the antiferromagnetic spin alignment.[38] This can also be explained on the basis of eq 5.4, where due to gain in S value the negative part dominates over the positive value of exchange. On the other hand, for the complex 2 the distances between closest S atoms of two separate layers are 3.76Å and 3.65Å respectively. Unlike complex 1, the HOMO diagram in complex 2 does not show any kind of overlap between donor and acceptor units. In spite of this zero overlap, the complex shows antiferromagnetic interaction which must operate through-space.

Table 5.3 The Antiferromagnetic Stacking Mode of the Complexes 1 and 2 and Their Rotational Angle, Lowest S-S Distance, Magnetic Exchange Coupling Constant (J) Value and HOMO-LUMO Picture in Their Singlet State at UB3LYP/LANL2DZ level

Complex	Rotational Angle (lowest S-S distance) (Coupling constant in cm^{-1})	HOMO
1	43°(3.62) ($J = -32$)	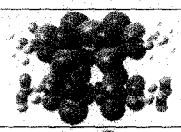
	67°(3.63) ($J = -35$)	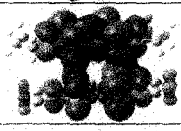
2	66°(3.76) ($J = -13$)	
	70°(3.65) ($J = -2$)	

Table 5.4 Occupation Numbers of DOMO, SOMOs and LUMO as well as T_{SOMO} for the Complexes in Singlet States and J Values Calculated by CASSCF(4,4) Method Using LANL2DZ Basis Set

Complex	θ	DOMO	SOMO1	SOMO2	LUMO	T_{SOMO}
(HMTTF)[Ni(mnt)$_2$]	43	1.85576	1.78618	0.20882	0.15085	0.80
	67	1.93751	1.53146	0.46922	0.06181	0.54
(ChSTF)[Ni(mnt)$_2$]	66	1.93807	1.00677	0.99356	0.06159	0.01
	70	1.93879	1.00053	0.99948	0.06120	0.01

In an interesting work, Butcher et al. show that two halide super exchange pathway for antiferromagnetic interaction between two magnetic sites may even occur through-space due to the spin delocalization from magnetic sites to the halogen atoms.[48] In the present work, we observe that the spin density is delocalized over the S atoms for these complexes. Thus in case of complex 2 the antiferromagnetic mode is not favored by covalent interaction rather it is due to through-space spin exchange. The extent of overlap (T_{SOMO}) between SOMOs (Table 5.4) in both the complexes also validates the HOMO diagram (Table 5.3) and rationalizes the degree of antiferromagnetic interaction. In antiferromagnetic stacking modes, Complex 1 has higher overlap between magnetic orbitals in comparison with complex 2 and expectedly displays more antiferromagnetic interaction than complex 2.

5.4 Conclusions

Intermolecular charge transfer brings versatile properties in mixed stack CT complexes; as a result they are very useful for different technological applications. DFT calculations are performed on two similar kind of mixed-stack complexes to elucidate the origin of the ferromagnetic interaction therein. The parallel spin alignment in the ground state of both the complexes stems from the transfer of a spin from β –HOMO of neutral donor (D) to the β-LUMO of neutral acceptor (A), which is expected because Ni(II) d orbitals already occupied by α electrons, are only susceptible for β electron acceptance. These parallel spins undergo through-space direct exchange to set in ferromagnetism in complex 1 and 2. And thus speak for obvious contribution from Ni(mnt)$_2$ fragment to magnetic interaction as claimed in reference 20 through

the larger g value than should be for TTF or STF only. The through-space nature of exchange is ensured from the zero value of overlap between magnetic orbitals. Both the complexes exhibit similar value of exchange coupling constant. This observation has been explained through comparable value of spin density on magnetic sites and S-S distance between two layers. Next, the geometry of the complexes is altered by changing the rotational angle between the layers. The plot of J against different rotational angle divulges maximum degree of ferromagnetic interaction in their minimum energy state for which the crystallographic file format is available. To search the reason of antiferroamgnetic behavior in some particular stacking modes, the MO diagram of the complexes is analyzed. The HOMO in complex 1 at rotational angle 43° and 67°, depicts a strong overlap between the magnetic orbitals which also finds its support from the significant T_{SOMO} value. This overlap, in its turn, induces antiparallel spin alignment causing antiferromagnetic interaction. The stronger overlap between the donor and acceptor in antiferromagnetic stacking modes compared to that in the ferromagnetic ground state is visible from their atom-atom overlap-weighted bond order (Appendix 1). On the other hand, complex 2 does not show such overlap, still behaves antiferromagnetically at rotational angles 66° and 70°. This is attributed to the through-space antiferromagnetic exchange. This wide variety of exchange mechanisms in complex 1 and 2, in their ferromagnetic ground state and antiferromagnetic states is schematized in scheme 5.1.

5.5 References

1. (a) Miller, J. S.; Epstein, A. J.; Reiff, W. M. *Chem. Rev.* **1988**, *88* , 201; (b) Enoki, T.; Miyazaki, A. *Chem. Rev.* **2004**, *104*, 5449; (c) Coronado, E.; Day, P. *Chem. Rev.* **2004**, *104*, 5419.

2. McConnell, H. M. *J. Chem. Phys.* **1963**, *39*, 1910.

3. Ishiguro, T.; Yamaji, K.; Saito, G. *Organic Superconductors*, 2nd ed. (Springer-Verlag, Berlin, 1998)

4. (a) Tokura, Y.; Okamoto, H.; Koda, T.; Mitani, T.; Saito, G. *Phys. Rev. B* **1991,** *43*, 8224. (b) Iwasa, Y.; Koda, T.; Koshihara, S.; Tokura, Y.; Iwasawa, N.; Saito, G. *Phys. Rev. B* **1989**, *39*, 10441.

5. Hasegawa, T.; Akutagawa, T.; Nakamura, T.; Sasou, Y.; Kondo, R.; Kagoshima, S.; Mochida, T.; Saito, G.; Iwasa, Y. *Synth. Met.* **1999**, *103*, 1804.

6. Hasegawa, T.; Akutagawa, T.; Nakamura, T. *Synth. Met.* **2003**, *133*, 623.

7. Kuwata-Gonokami, M.; Peyghambarian, N.; Meissner, K.; Fluegel, B.; Sato, Y.; Ema, K.; Shimano, R.; Mazumdar, S.; Guo, F.; Tokihiro, T.; Ezaki, H.; Hanamura, E. *Nature* **1994**, *367*, 47.

8. Aoki, S.; Nakayama, T.; Miura, A. *Phys. Rev. B* **1993**, *48*, 626.

9. Chiang, L. Y.; Upasani, R. B.; Goshorn, D. P.; Swirczewski. J. W. *Chem. Mater.* **1992**, *4*, 394.

10. (a) Tormos, G. V.; Bakker, M. G.; Wang. P.; Lakshmikantam, M. V.; Cava, M. P.; Metger, R. M. *J. Am. Chem. Soc.* **1995**, *117*, 8528. (b) Ren, X.; Lu, C.; Liu, Y.; Zhu, H.; Li, H.; Hu, C.; Meng, Q. *Transition Met. Chem.* **2001**, *26*, 136. (c) Gutlich, P.; Garcia, Y.; Woike, T. *Coord. Chem. Rev.* **2001**, *219*, 839. (d) Breslow, R.; *Mol. Cryst. Liq. Cryst.*, 1985, **125**, 261. (e) LePage, T.; Breslow, R. *J. Am. Chem. Soc.* **1987**, *109*, 6412. (f) Miller, J. S.; Epstein, A. J.; *Ferromagnetic Exchange in Molecular Solids*; NATO AS1 Series (Series B, Physics) 168; Plenum: New York, 1987. (g) Chittipeddi, S. R.; Epstein, A. J.; Zhang, J. H.; Reiff, W. M.; Hamberg, I.; Tanner, D. B.; Johnson, D. C.; Miller, J. S. *Synth. Met.* **1988**, *19*, 731. (h) Mas-Torrent, M.; Alves, H.; Lopes, E. B.; Almeida, M.; Wurst, K.; Vidal-Gancedo, J.; Veciana, J.; Rovira, C. *J. Solid State Chem.* **2002**, *168*, 563.

11. (a) Simonsen, K, B.; Zong, K.; Rogers, R. D.; CavaJan Becher, M. P. C. *J. Org. Chem.* **1997**, *62*, 679. (b) Cooke, G.; de Cremiers, H. A.; Duclairoir, F. M. A.; Gray, M.; Vaqueiro, P.; Powell, A. V.; Rosair, G.; Rotello, V. M. *Tet. Lett.* **2001**, *42*, 5089.

12. McConnell, H. M. *Proc. Robert A. Welch Found. Conf. Chem. Res.* **1967**, *11*, 144.

13. Radhakrishnan, T. P.; Soos, Z. G.; Endres, H.; Azevado, L. J. *J. Chem. Phys.* **1986**, *85*, 1126.

14. Breslow, R.; Jaun, B.; Kluttz, R. Q.; Xia, C. *Tetrahedron* **1982**, *38*, 863.

15. Miller, J. S.; Epstein, A. J. *J. Am. Chem. Soc.* **1987**, *109*, 3850.

16. Yamaguchi, K.; Toyoda, Y.; Fueno, T. *Chem. Phys. Lett.* **1989**, *159*, 459.

17. Takano, Y.; Taniguchi, T.; Isobe, H.; Kubo, T.; Morita, Y.; Yamamoto, K.; Nakasuji, K.; Takui, T.; Yamaguchi, K. *J. Am. Chem. Soc.* **2002**, *124*, 11122.

18. Ni, Z.; Ren, X.; Ma, J.; Xie, J.; Ni, C.; Chen, Z.; Meng, Q. *J. Am. Chem. Soc.* **2005**, *127*, 14330.

19. Devic, T.; Domercq, B.; Auban-Senzier, P.; Molinie, P.; Fourmigue, M. *Eur. J. Inorg. Chem.*, **2002**, 2844.

20. Nakajima, H.; Katsuhara, M.; Ashizawa, M.; Kawamoto, T.; Mori, T. *Inorg. Chem.*, **2004**, *43*, 6075.

21. (a) Epstein, A. J.; Chittipeddi, S.; Chakraborty, A.; Miller, J. S. *J. Appl. Phys.* **1988**, *63*, 2952. (b) Weiss, E. A.; Tauber, M. J.; Ratner, M. A.; Wasielewski, M. R. **2005**, *127*, 6052.

22. Newton, M. D. *Chem. Rev.* **1991**, *91*, 767.

23. (a) Weiss, E. A.; Wasielewski, M. R.; Ratner, M. A. *J. Chem. Phys.* **2005**, *123*, 064504. (b) Lopez-Castillo, J. M.; Jay-Gerin, J. P. *J. Phys. Chem.* **1996**, *100*, 14289.

24. Gruschus, J. M.; Kuki, A. *J. Phys. Chem.* **1993**, *97*, 5581.

25 (a) Wells, M. C.; Lucchese, R. R. *J. Comput. Chem.* **2000**, *21*, 1262. (b) Bicout, D. J.; Kats, E. *Phys. Lett. A* **2002,** *300*, 479.

26. (a) Yamaguchi, K.; Takahara, Y.; Fueno, T.; Nasu, K. *Jpn. J. Appl. Phys.* **1987**, *26*, L1362. (b) Yamaguchi, K.; Jensen, F.; Dorigo, A.; Houk, K. N. *Chem. Phys. Lett.* **1988**, *149*, 537. (c) Yamaguchi, K.; Takahara, Y.; Fueno, T.; Houk, K. N.; *Theor. Chim. Acta* **1988**, *73*, 337.

27. **(a)** Yoshizawa, K.; Hoffmann, R. *J. Am. Chem. Soc.* **1995**, *117*, 6921. (b) de P. R. Moreira I.; Illas, F. *Phys. Chem. Chem. Phys.* **2006,** *8*, 1645.

28. (a) Noodleman, L. *J. Chem. Phys.* **1981**, *74*, 5737. (b) Noodleman, L.; Baerends, E. J. *J. Am. Cmem. Soc.*, **1984**, *106*, 2316.

29. (a) Bencini, A.; Totti, F.; Daul, C. A.; Doclo, K.; Fantucci, P.; Barone, V. *Inorg. Chem.*, **1997**, *36*, 5022. (b) Bencini, A.; Gatteschi, D.; Totti, F.; Sanz, D. N.; McClevrty, J. A.; Ward, M. *J. Phys. Chem. A* **1998**, *102*, 10545.

30. Ruiz, E.; Cano, J.; Alvarez, S.; Alemany, P. *J. Comput. Chem.* **1999**, *20*, 139.

31. (a) Polo, V.; Alberola, A.; Andres, J.; Anthony, J.; Pilkington, M. *Phys. Chem. Chem. Phys.* **2008**, *10*, 857. (b) Bhattacharya, D.; Misra, A. *J. Phys. Chem. A* **2009**, *113*, 5470. (c) Paul, S.; Misra, A. *J. Mol. Str. (THEOCHEM)* **2009**, *907*, 35. (d) Paul, S.; Misra, A. *J. Mol. Str. (THEOCHEM)* **2009**, *156*, 895. (e) Bhattacharya, D.; Shil, S.; Panda, A.; Misra, A. *J. Phys. Chem. A* **2010**, *114*, 11833. (e) Paul, S.; Misra, A. *J. Phys. Chem. A* **2010**, *114*, 6641; (f) Bhattacharya, D.; Shil, S.; Misra, A.; Klein, D. J. *Theor. Chem. Acc.* **2010**, *127*, 57. (g) Paul, S.; Misra, A. *J. Chem. Theor. Comput.* **2012**, *8*, 843.

32. Galperin, M.; Segal, D.; Nitzam, A. *J. Chem. Phys.* **1999**, *111*, 1569.

33. (a) Anderson, P. W. *Phys. Rev.* **1950**, *79*, 350. (b) Anderson, P. W. *Phys. Rev.* **1959**, *115*, 2. (c) Anderson, P. W. in Theory of the Magnetic Interaction: Exchange in Insulators and

Superconductors, *Solid State Physics* Vol. 14, edited by F. Turnbull, and F. Seitz, Academic, New York, 1963, p. 99.

34. (a) Munoz, D.; Illas, F.; de P. R. Moreira I. *Phys. Rev. Lett.* **2000**, *84*, 1579. (b) Caballol, R.; Castell, O.; Illas, F.; Moreira, I. de P. R.; Malrieu, J. P. *J. Phys. Chem. A* **1997**, *101*, 7860-7866.

35. (a) Calzado, C. J.; Cabrero, J.; Malrieu, J. P.; Caballol, R. *J. Chem. Phys.* **2002**, *116*, 2728. (b) Calzado, C. J.; Cabrero, J.; Malrieu, J. P.; Caballol, R. *J. Chem. Phys.* **2002**, *116*, 3985. (c) Calzado, C. J.; Angeli, C.; Taratiel, D.; Caballol, R.; Malrieu, J. P. *J. Chem. Phys.* **2009**, *131*, 044327.

36. Paul, S.; Misra, A. *J. Chem. Theory and Comput.* **2012**, *8*, 843.

37. Kollmar, C.; Kahn, O. *Acc. Chem. Res.* **1993**, *26*, 259.

38. Takano, Y.; Kitagawa, Y.; Onishi, T.; Yoshioks, Y.; Yamaguchi, K.; Koga, N.; Iwamura, H. *J. Am. Chem. Soc.* **2002**, *124*, 450.

39. (a) Mitani, M.; Takano, Y.; Yoshioka, Y.; Yamaguchi, K. *J. Chem. Phys.* **2000**, *113*, 4035. b) Mitani, M.; Takano, Y.; Yoshioka, Y.; Yamaguchi, K. *J. Chem. Phys.* **1999**, *111*, 1309. (c) Shil, S.; Misra, A. *J. Phys. Chem. A* **2010**, *114*, 2022. (d) Bhattacharya, D.; Shil, S.; Misra, A. *J. Photochem. Photobiol. A: Chem* **2011**, *217*, 402.

40. (a) Yang, Y.; Weaver, M. N.; Merz, Jr. K. M. *J. Phys. Chem. A* **2009**, *113*, 9843. (b) Chiodo, S.; Russo, N.; Sicilia, E. *J. Chem. Phys.* **2006**, *125*, 104107.

41. (a) Wang, B.; Wei, H.; Wang, M.; Chen, Z. *J. Chem. Phys.*, **2005**, *122*, 204310. (b) Mödl, M.; Dolg, M.; Fulde, P.; Stoll, H. *J. Chem. Phys.*, **1997**, *106*, 1836.

42. Pulay, P.; Hamilton, T. P. *J. Chem. Phys.* **1988**, *88*, 4926.

43. Gaussian 09, Revision **A.1**, Frisch, M. J.; Trucks, G. W.; Schlegel, H. B.; Scuseria, G. E.; Robb, M. A.; Cheeseman, J. R.; Scalmani, G.; Barone, V.; Mennucci, B.; Petersson, G. A.; Nakatsuji, H.; Caricato, M.; Li, X.; Hratchian, H. P.; Izmaylov, A. F.; Bloino, J.; Zheng, G.; Sonnenberg, J. L.; Hada, M.; Ehara, M.; Toyota, K.; Fukuda, R.; Hasegawa, J.; Ishida, M.; Nakajima, T.; Honda, Y.; Kitao, O.; Nakai, H.; Vreven, T.; Montgomery, Jr., J. A.; Peralta, J. E.; Ogliaro, F.; Bearpark, M.; Heyd, J. J.; Brothers, E.; Kudin, K. N.; Staroverov, V. N.; Kobayashi, R.; Normand, J.; Raghavachari, K.; Rendell, A.; Burant, J. C.; Iyengar, S. S.; Tomasi, J.; Cossi, M.; Rega, N.; Millam, N. J.; Klene, M.; Knox, J. E.; Cross, J. B.; Bakken, V.; Adamo, C.; Jaramillo, J.; Gomperts, R.; Stratmann, R. E.; Yazyev, O.; Austin, A. J.; Cammi, R.; Pomelli, C.; Ochterski, J. W.; Martin, R. L.; Morokuma, K.; Zakrzewski, V. G.; Voth, G. A.; Salvador, P.;

Dannenberg, J. J.; Dapprich, S.; Daniels, A. D.; Farkas, Ö.; Foresman, J. B.; Ortiz, J. V.; Cioslowski, J.; Fox, D. J. Gaussian, Inc., Wallingford CT, 2009.

44. Zhuldev, A.; Barone, V.; Bonnet, M.; Delley, B.; Grand, A.; Ressouche, E.; Rey, P.; Subra, R.; Schweizer, J. *J. Am. Chem. Soc.* **1994,** *116*, 2019.

45. Huyett, J. E.; Choudhury, S. B.; Eichhorn, D. M.; Bryngelson, P. A.; Maroney, M. J.; Hoffman, B. M. *Inorg. Chem.* **1998**, *37*, 1361.

46. (a) Reed, A. E.; Curtiss, L. A.; Weinhold, F. *Chem. Rev.* **1988**, *88*, 899. (b) Montejo, M.; Navarro, A.; Kearley, G. J.; Va´zquez, J.; Lo´pez-Gonza´lez, J. J. *J. Am. Chem. Soc.* **2004**, *126*, 15087.

47. Hansong Cheng, H.; Wang, L. S. *Phys. Rev. Lett.* **1996**, *77*, 51.

48. Butcher, R. T.; Novoa, J. J.; Ribas-Ariño, J.; Sandvik, A. W.; Turnbull, M. M.; Landee, C. P.; Wells, B. M.; Awaddi, F. F. *Chem. Comm.*, **2009**, 1359.